

## The Potential Distribution at the Semiconductor/Solution Interface

Arun Natarajan, Gerko Oskam, and Peter C. Searson\*

Department of Materials Science and Engineering, The Johns Hopkins University, Baltimore, Maryland 21218

Received: January 28, 1998; In Final Form: May 23, 1998

In semiconductor electrochemistry there is considerable confusion concerning the potential distribution at the semiconductor/solution interface under weak depletion and accumulation conditions. The applied potential is partitioned between the space charge layer in the semiconductor and the Helmholtz layer on the solution side of the interface. Under deep depletion conditions, a change in the applied potential usually appears across the space charge layer and the band bending can be determined using the Mott–Schottky relation. Under conditions of weak depletion or accumulation, however, the applied potential is partitioned between the two double layers and determination of band bending is not straightforward. In this paper, expressions for the dependence of the band bending on the applied potential are derived and the consequences for charge-transfer processes are discussed.

### Introduction

When a semiconductor is brought into contact with a solution containing a redox couple, thermodynamic equilibrium is established when the electrochemical potentials of species that can be exchanged between both phases are equal. In most cases, only electrons can be exchanged between the semiconductor and the solution and charge flows across the interface until the Fermi energy of the semiconductor is aligned with the equilibrium energy of the solution. The charge build up on both sides of the interface leads to a potential drop over the space charge layer in the semiconductor and the Helmholtz layer on the solution side of the interface. On imposing an externally applied potential, the equilibrium is perturbed and the potential distribution across the interface changes. To determine the thermodynamic properties of the semiconductor/solution interface, or kinetic parameters associated with charge transfer across the interface it is necessary to determine how the applied potential is partitioned between the space charge layer and the Helmholtz layer.<sup>1–4</sup>

There are two limiting cases for the partitioning of the applied potential: (i) any change in applied potential is dropped across the space charge layer and (ii) any change in applied potential appears across the Helmholtz layer. This situation is often discussed<sup>1–4</sup> in terms of an equivalent circuit where the interface is modeled as two capacitors in series corresponding to the space charge layer capacitance ( $C_{sc}$ ) and the Helmholtz layer capacitance ( $C_H$ ). Additional capacitors representing charge stored in surface states or adsorbates may also be included. It follows that any change in the applied potential will be dropped across the region with the smallest capacity, leading to the two limiting cases described above. For  $C_{sc} \ll C_H$ , any change in applied potential is dropped across the space charge layer, whereas for  $C_H \ll C_{sc}$ , any change in applied potential appears across the Helmholtz layer. These two situations correspond to deep depletion and accumulation respectively. In practice, however, the intermediate case is also of interest since this corresponds to the potential regime from weak depletion to weak accumulation, and represents the transition from the situation where the position of the band edges at the surface are fixed to the case where the band edges are completely unpinned. Although the

transition between these two limiting cases has been described qualitatively in the literature,<sup>1–4</sup> there are no theoretical treatments describing the partitioning of the applied potential in this regime.

When a depletion layer is formed at the semiconductor surface, the space charge layer capacitance is smaller than the Helmholtz layer capacitance and a change in the applied potential appears across the space charge layer. In this regime, the interfacial capacitance corresponds to the space charge layer capacitance and the Mott–Schottky relation can be used to determine the band bending as a function of the applied potential and, hence, the position of the band edges at the surface.<sup>5–12</sup> The other limiting case, when the space charge layer capacitance is larger than the Helmholtz capacitance, has not received much attention. Under these conditions, it is not straightforward to determine the band bending. Indeed, there is considerable confusion in the literature concerning the potential distribution at potentials close to the flat band potential.

In this paper, we consider the partitioning of the applied potential in weak depletion and accumulation and derive expressions that describe the partitioning under both steady-state and non-steady-state conditions. We show that charge build up at the semiconductor surface at potentials close to the flat band potential is sufficient to lead to unpinning of the band edges. At potentials negative to the flat band potential, the band bending asymptotically approaches a limiting value corresponding to the formation of a weak accumulation layer. Further, we show how the partitioning influences the measured capacitance in this potential regime. Finally, we discuss the implications of the partitioning on kinetic analysis of charge-transfer processes at the semiconductor/solution interface.

### Partitioning of the Applied Potential

Figure 1 shows an energy-band diagram for an  $n$ -type semiconductor in contact with a solution. In the following analysis, we derive expressions for the case where the applied potential is partitioned between the space charge layer and the Helmholtz layer, as shown in Figure 1. The influence of interfacial layers (such as oxides), electrically active surface

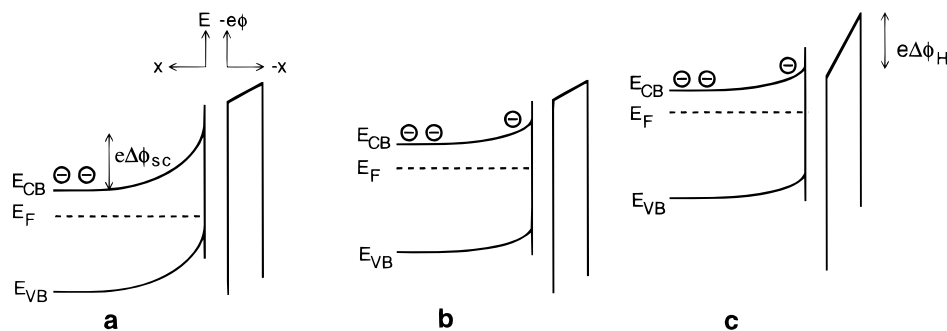


**Figure 1.** (a) Energy-band diagram for an n-type semiconductor/solution interface under depletion conditions in the dark illustrating the potential drop across the space charge layer and the potential drop across the Helmholtz layer. A change in the applied potential can result in (b) a change in the band bending or (c) a change in the potential drop across the Helmholtz layer and unpinning of the band edges.

states, and diffuse double layers in the solution is also discussed, and the analysis can be readily extended to include these features.

The total potential drop across the interface,  $\Delta\phi_{\text{total}}$ , is given by<sup>1-4</sup>

$$\Delta\phi_{\text{total}} = \Delta\phi_{\text{sc}} + \Delta\phi_{\text{H}} \quad (1)$$

where  $\Delta\phi_{\text{sc}}$  is the potential drop across the semiconductor space charge layer and  $\Delta\phi_{\text{H}}$  is the potential drop across the Helmholtz layer.  $\Delta\phi_{\text{sc}}$  is defined as

$$\Delta\phi_{\text{sc}} = \phi_{\text{sc}}^{\text{s}} - \phi_{\text{sc}}^{\text{b}} \quad (2)$$

where  $\phi_{\text{sc}}^{\text{s}}$  is the electrostatic potential at the surface and  $\phi_{\text{sc}}^{\text{b}}$  is the potential in the bulk. The potential drop across the Helmholtz layer is given by

$$\Delta\phi_{\text{H}} = \phi_{\text{soln}} - \phi_{\text{sc}}^{\text{s}} \quad (3)$$

where  $\phi_{\text{soln}}$  is the potential of the bulk solution. The electrostatic potential drops at the interface can be related to the applied potential,  $U$ , by choosing an appropriate reference. In semiconductor electrochemistry, the applied potential is generally referenced to the potential where the bands are flat,  $U_{\text{fb}}^0$ .<sup>13</sup> In the absence of an interfacial layer or electrically active surface states,  $\Delta\phi_{\text{sc}} = \Delta\phi_{\text{H}} = 0$ <sup>14</sup> at an applied potential  $U = U_{\text{fb}}^0$ , and we obtain

$$U - U_{\text{fb}}^0 = \phi_{\text{sc}}^{\text{b}} - \phi_{\text{soln}} = -\Delta\phi_{\text{total}} \quad (4)$$

Experimentally, the flat band potential,  $U_{\text{fb}}$ , is usually obtained by extrapolation from the capacitance in deep depletion.<sup>5-12</sup> In some cases, however, the value for the flat band potential obtained by this method is not equal to  $U_{\text{fb}}^0$  (i.e.  $\Delta\phi_{\text{sc}} \neq 0$  when  $U = U_{\text{fb}}$ ) due to unpinning of the band edges in the weak depletion regime. This is shown schematically in Figure 1. Band-edge unpinning can occur as a result of surface reactions (e.g., conversion of hydrogen-terminated to hydroxyl-terminated surface),<sup>15-17</sup> filling and emptying of surface states,<sup>18-29</sup> charging of an interfacial layer,<sup>30-33</sup> or partitioning of the applied potential as  $C_{\text{sc}}$  approaches the value of  $C_{\text{H}}$ .<sup>1-4,10,11,34</sup>

First we derive an expression for the partitioning of the applied potential under steady-state (dc) conditions. It is convenient to define the dc potential drop over the space charge layer as a function of the dc applied potential in terms of the coefficient  $\gamma_{\text{dc}}$

$$\gamma_{\text{dc}} = \frac{-\Delta\phi_{\text{sc}}}{U - U_{\text{fb}}^0} \quad (5)$$

The fraction of the applied potential dropped across the space charge layer can be obtained from the conservation of charge. For the case where there is no charge trapped in interface states or interfacial layers

$$Q_{\text{sc}} + Q_{\text{H}} = 0 \quad (6)$$

The charge in the Helmholtz layer,  $Q_{\text{H}}$ , can be obtained from the Helmholtz layer capacitance and the potential drop over the Helmholtz layer. If it is assumed that the differential Helmholtz layer capacitance ( $C_{\text{H}} = |dQ_{\text{H}}/d\Delta\phi_{\text{H}}|$ ) is independent of  $\Delta\phi_{\text{H}}$ ,<sup>2,10,35-37</sup>

$$Q_{\text{H}} = C_{\text{H}}\Delta\phi_{\text{H}} = -C_{\text{H}}((U - U_{\text{fb}}^0) + \Delta\phi_{\text{sc}}) \quad (7)$$

The total charge in the semiconductor space charge layer,  $Q_{\text{sc}}$ , is proportional to the electric field at the surface,  $\xi^{\text{s}}$ , and can be obtained from Gauss' law and the Poisson–Boltzmann equation<sup>7</sup>

$$Q_{\text{sc}} = \epsilon\epsilon_0\xi^{\text{s}} = \mp(2kT\epsilon\epsilon_0N_{\text{D}})^{1/2}\left(\exp\left(\frac{e\Delta\phi_{\text{sc}}}{kT}\right) - \frac{e\Delta\phi_{\text{sc}}}{kT} - 1\right)^{1/2} \quad (8)$$

where  $\epsilon$  is the relative permittivity,  $\epsilon_0$  is the permittivity of free space,  $e$  is the electronic charge,  $N_{\text{D}}$  is the donor density (for an n-type semiconductor assuming complete ionization),  $k$  is the Boltzmann constant, and  $T$  is the temperature. The minus sign corresponds to accumulation ( $\Delta\phi_{\text{sc}} > 0$ ), where the excess charge is due to excess conduction band electrons, and the positive sign corresponds to depletion ( $\Delta\phi_{\text{sc}} < 0$ ), where the excess charge is due to ionized donors.

Inserting eqs 7 and 8 into eq 6 we obtain

$$-C_{\text{H}}((U - U_{\text{fb}}^0) + \Delta\phi_{\text{sc}}) \mp (2N_{\text{D}}\epsilon\epsilon_0kT)^{1/2}\left(\exp\left(\frac{e\Delta\phi_{\text{sc}}}{kT}\right) - \frac{e\Delta\phi_{\text{sc}}}{kT} - 1\right)^{1/2} = 0 \quad (9)$$

The band bending,  $e\Delta\phi_{\text{sc}}$ , can be determined from eq 9 as a function of the applied potential for given values of  $C_{\text{H}}$ . Figure 2 shows a plot of  $\gamma_{\text{dc}}$  versus the applied potential calculated for a semiconductor with  $N_{\text{D}} = 10^{15} \text{ cm}^{-3}$  and  $\epsilon = 12$  and a Helmholtz layer capacitance of  $1 \mu\text{F cm}^{-2}$ . We note that values of about  $1-3 \mu\text{F cm}^{-2}$  have been reported in the literature for the magnitude of the Helmholtz capacitance at semiconductor surfaces.<sup>30,38-40</sup> At potentials positive to the flat band potential, where the surface is in weak depletion,  $\gamma_{\text{dc}}$  asymptotically approaches 1.0. At potentials negative of the flat band potential,  $\gamma_{\text{dc}}$  decreases sharply, illustrating that the band edges become unpinned and most of the applied potential is dropped over the Helmholtz layer.

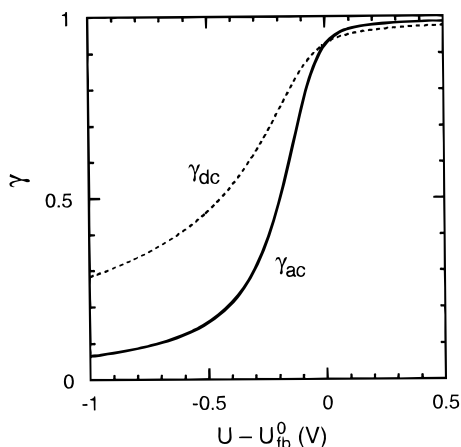


**Figure 2.** Fraction of the applied potential  $\gamma_{dc}$  dropped over the space charge layer under steady-state conditions versus the applied potential ( $U - U_{fb}^0$ ) calculated for  $\epsilon = 12$ ,  $N_D = 1 \times 10^{15} \text{ cm}^{-3}$ , and  $C_H = 1 \mu\text{F cm}^{-2}$ . The fraction of the differential applied potential,  $\gamma_{ac}$ , dropped over the space charge layer is also shown.

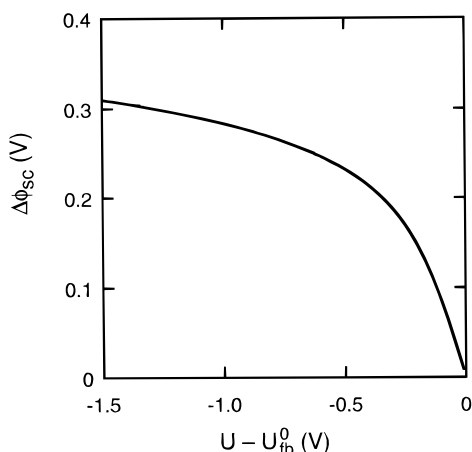


**Figure 3.** Band bending  $\Delta\phi_{sc}$  versus applied potential ( $U - U_{fb}^0$ ) calculated for  $\epsilon = 12$ ,  $N_D = 1 \times 10^{15} \text{ cm}^{-3}$ , and  $C_H = 1 \mu\text{F cm}^{-2}$ .

Figure 3 shows the band bending  $\Delta\phi_{sc}$  versus the applied potential calculated using the same values for  $N_D$ ,  $\epsilon$ , and  $C_H$ . From this figure it can be seen that the band bending is proportional to the applied potential in depletion but approaches a limiting value of about 300 mV in the accumulation regime.

We now consider the partitioning of the applied potential under non-steady-state conditions. This is important for experimental measurements involving a small transient or periodic perturbation of the applied potential. At any applied potential,  $U$ , a change in the applied potential,  $dU$ , is partitioned over the space charge layer and the Helmholtz layer

$$-dU = d(\Delta\phi_{\text{total}}) = d(\Delta\phi_{sc}) + d(\Delta\phi_H) \quad (10)$$

The fraction of the applied potential,  $dU$ , dropped across the space charge layer can be described in terms of the coefficient  $\gamma_{ac}$

$$\gamma_{ac} = -\frac{d(\Delta\phi_{sc})}{dU} \quad (11)$$

where  $\gamma_{ac}$  is between 0 and 1. From eqs 10 and 11 it follows that

$$1 - \gamma_{ac} = -\frac{d(\Delta\phi_H)}{dU} \quad (12)$$

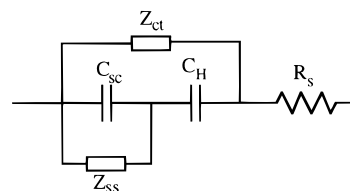


**Figure 4.** Equivalent circuit for the semiconductor/solution interface valid for situations where the dc current is small and the density of surface states is low.

From eqs 10–12 and the conservation of charge, it can be easily shown that

$$\gamma_{ac} = \frac{C_H}{C_H + C_{sc}} \quad (13)$$

where  $C_{sc}$  is the differential space charge layer capacitance ( $C_{sc} = |dQ_{sc}/d(\Delta\phi_{sc})|$ ). Equation 13 shows that  $\gamma_{ac}$  is independent of frequency. However, processes such as filling and emptying of surface states may lead to a frequency dependence.

Figure 2 shows that  $\gamma_{ac}$  also decreases at applied potentials negative to the flat band potential. Furthermore,  $\gamma_{ac}$  decreases to values close to 0, corresponding to the case where any change in applied potential is dropped across the Helmholtz layer.

From eqs 5 and 11 it can be seen that the parameter  $\gamma_{ac}$  is related to  $\gamma_{dc}$

$$\gamma_{ac} = \gamma_{dc} + (U - U_{fb}^0) \frac{d\gamma_{dc}}{dU} \quad (14)$$

Both  $\gamma_{ac}$  and  $\gamma_{dc}$  are essential parameters for the analysis of charge-transfer kinetics at the semiconductor/solution interface. The parameter  $\gamma_{ac}$  is important in the analysis of measurements involving a small transient or a periodic perturbation technique, such as electrochemical impedance spectroscopy. In addition,  $\gamma_{ac}$  determines the slope of current–potential curves, as described in a subsequent section. The parameter  $\gamma_{dc}$  is important in analyzing the kinetics of reactions under steady-state conditions where the reaction rate may be dependent on the magnitude of the band bending or the overpotential.

### Total Capacitance

Impedance spectroscopy and, in particular, capacitance measurements are routinely used to determine the position of the band edges and the band bending as a function of the applied potential.<sup>2,8,11,12,18,19</sup> To analyze the impedance response of a semiconductor/electrolyte interface, it is usually necessary to have an equivalent circuit model of the interface so that the space charge layer capacitance can be extracted from the measured capacitance as a function of frequency. In this section, we derive the relation between the partitioning of the applied potential and the interfacial capacitance in the potential regime close to the flat band potential.

Figure 4 shows the equivalent circuit generally used for analysis of the impedance response of the semiconductor/solution interface.<sup>2,41</sup> The total interfacial capacitance for the equivalent circuit shown in Figure 4 is given by

$$C_{\text{total}} = \frac{C_{sc}C_H}{C_{sc} + C_H} \quad (15)$$

To extract  $C_{sc}$  from  $C_{\text{total}}$ , it is necessary to determine the dependence of  $C_{sc}$  on the applied potential. Since  $C_{sc}$  is dependent on the band bending,  $\Delta\phi_{sc}$ , the partitioning of the

applied potential must be also be known. Below we show how this case can be analyzed.

An expression for  $C_{sc}$  can be obtained by differentiation of eq 8

$$C_{sc} = \left( \frac{e^2 N_D \epsilon_0}{2kT} \right)^{1/2} \left[ \exp\left(\frac{e\Delta\phi_{sc}}{kT}\right) - 1 \right] \left[ \exp\left(\frac{e\Delta\phi_{sc}}{kT}\right) - \frac{e\Delta\phi_{sc}}{kT} - 1 \right]^{-1/2} \quad (16)$$

At sufficiently large band bending in the depletion regime ( $\Delta\phi_{sc} < -3kT/e$ ), eq 16 reduces to the Mott–Schottky relation<sup>2</sup>

$$C_{sc} = \left( \frac{e^2 N_D \epsilon_0}{2kT} \right)^{1/2} \left( -\frac{e\Delta\phi_{sc}}{kT} - 1 \right)^{-1/2} \quad (17)$$

Under depletion conditions, the differential space charge layer capacitance for a moderately doped semiconductor is usually much smaller than the Helmholtz layer capacitance and a change in the applied potential results in an equal change in the band bending. Under these conditions,  $\Delta\phi_{sc} = -(U - U_{fb})$  and the measured capacitance,  $C$ , is equal to  $C_{sc}$  so that eq 17 can be rewritten as

$$\frac{1}{C^2} = \left( \frac{2}{e N_D \epsilon_0} \right) \left( U - U_{fb} - \frac{kT}{e} \right) \quad (18)$$

Equation 18 is often used for the determination of the flat band potential,  $U_{fb}$ , and the donor density,  $N_D$ . The influence of factors such as surface roughness and the Helmholtz capacitance have been discussed in the literature.<sup>8,11,41–45</sup>

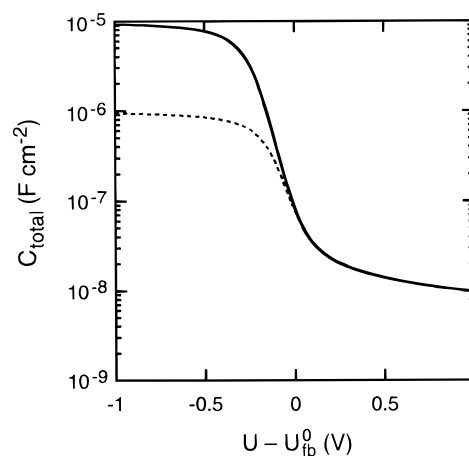
In the accumulation regime at sufficiently large band bending ( $\Delta\phi_{sc} > 3kT/e$ ), eq 16 reduces to

$$C_{sc} = \left( \frac{e^2 N_D \epsilon_0}{2kT} \right)^{1/2} \exp\left(\frac{e\Delta\phi_{sc}}{2kT}\right) = \left( \frac{e^2 N_D \epsilon_0}{2kT} \right)^{1/2} \exp\left(-\frac{e\gamma_{dc}(U - U_{fb}^0)}{2kT}\right) \quad (19)$$

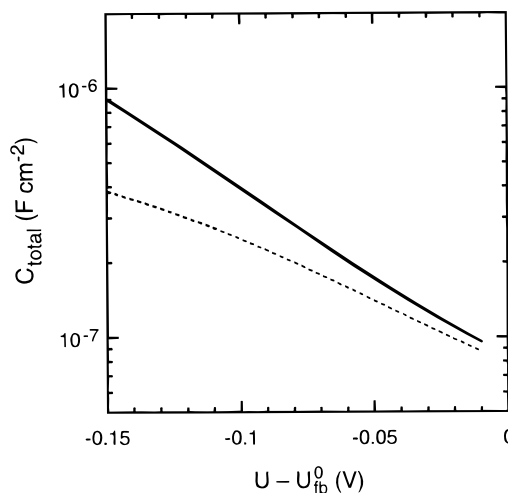
Under these conditions, it can be seen that the differential space charge layer capacitance is proportional to the exponential of the band bending with an inverse slope of 120 mV per decade.<sup>2,7,11,12</sup> We note that this expression is applicable as long as the Fermi level is below the position of the conduction band edge at the surface (i.e., weak accumulation), where the Boltzmann equation is valid.<sup>11</sup> For a donor density of  $10^{15} \text{ cm}^{-3}$ , this corresponds to a band bending of about 300 meV. Experimental verification of eq 19 is not straightforward since the dependence of  $\gamma_{dc}$  on the applied potential must be known.

Figure 5 shows a plot of  $C_{total}$  versus the applied potential obtained by solving eqs 9 and 16 for different values of the Helmholtz capacitance. In the depletion regime,  $C_{total} = C_{sc}$  since  $C_{sc} \ll C_H$  whereas at potentials close to the flat band potential and in the accumulation regime,  $C_{total}$  depends strongly on the value for  $C_H$  used in the calculations. Similar curves have been reported for the capacitance at  $\text{ZnO}$ <sup>11</sup> and  $\text{WSe}_2$ <sup>43</sup> surfaces.

Figure 6 shows  $C_{total}$  on a semilogarithmic plot in the potential range close to the flat band potential, illustrating that the inverse slope of the curves depends on the value of  $C_H$ . Figure 7 shows the dependence of the inverse slope on the Helmholtz capacitance. For sufficiently large values of  $C_H$ , the inverse slope is 120 mV per decade in this potential range, in accordance with eq 19. Thus, the slope of a plot of  $C_{total}$  versus applied potential



**Figure 5.** Calculated total capacitance versus applied potential ( $U - U_{fb}^0$ ) for  $\epsilon = 12$ ,  $N_D = 1 \times 10^{15} \text{ cm}^{-3}$ , and  $C_H = 10 \mu\text{F cm}^{-2}$  (—) and  $C_H = 1 \mu\text{F cm}^{-2}$  (···).



**Figure 6.** Calculated total capacitance in the potential regime close to the flat band potential for  $C_H = 10 \mu\text{F cm}^{-2}$  (—) and  $C_H = 1 \mu\text{F cm}^{-2}$  (···).

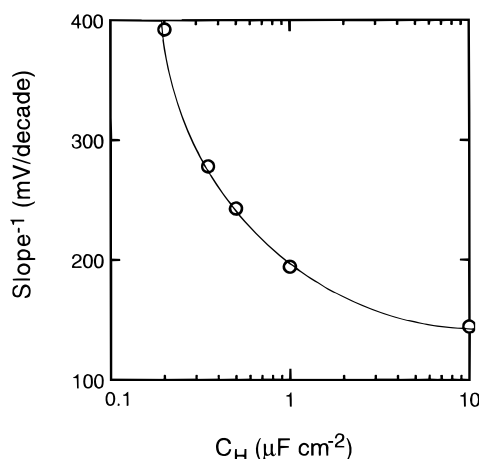


**Figure 7.** Inverse slope of the calculated total capacitance versus applied potential in the vicinity of the flat band potential for  $\epsilon = 12$  and  $N_D = 1 \times 10^{15} \text{ cm}^{-3}$  as a function of the Helmholtz capacitance.

at potentials slightly negative of the flat band potential can be used to estimate the magnitude of the Helmholtz capacitance.

Figure 8 shows results from microwave reflectivity measurements on n-type silicon in the potential range negative of the flat band potential. The microwave admittance is obtained from the modulated microwave response to a potential modulation



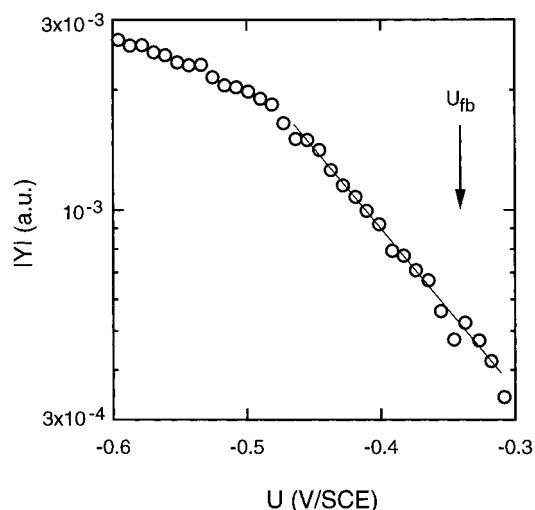


**Figure 8.** Microwave admittance  $|Y|$  versus applied potential in the accumulation regime for n-Si(100) in 1 M HF solution in the dark. The resistivity of the silicon, determined from four-point probe measurements, was  $5 \Omega \text{ cm}$  ( $N_D = 1 \times 10^{15} \text{ cm}^{-3}$ ). The microwave admittance,  $Y$ , is defined as  $\tilde{R}/\tilde{U}$ , where  $\tilde{R}$  is the modulated microwave reflectivity and  $\tilde{U}$  is the modulated potential. It can be shown that  $Y = S^*C_{\text{total}}$ , where  $S^*$  is the modified sensitivity factor.<sup>46</sup> The modulation amplitude was 10 mV (rms), and the frequency was 100 Hz. Other experimental details can be found in ref 46. The solid line corresponds to an inverse slope of 230 mV/decade.

and is proportional to the total capacitance.<sup>46</sup> The inverse slope of 230 mV/decade corresponds to a Helmholtz capacitance of about  $0.5 \mu\text{F cm}^{-2}$ . As described above, similar values for the Helmholtz capacitance at semiconductor surfaces have been reported in the literature.

### Current–Potential Curves

There has been significant interest in the determination of rate constants for electron transfer at semiconductor surfaces.<sup>47–60</sup> In this section, we show how the partitioning of the applied potential influences the determination of kinetic parameters associated with charge transfer at the semiconductor/solution interface.

For the specific case where a change in applied potential is dropped across the space charge layer, the Marcus–Gerischer model may be used to determine the rate constants.<sup>2,4,56,61–79</sup> This analysis can only be performed, however, if the following conditions are satisfied: (i) the surface electron concentration can be calculated from analysis of the position of the band edges in deep depletion (e.g., Mott–Schottky analysis), (ii) the energy of the redox couple is such that the current–potential curves can be analyzed in weak depletion (usually at least 200–300 mV from the flat band potential), (iii) the density of surface states is sufficiently low, and (iv) the surface is stable in the solution.

For systems that do not meet these requirements, kinetic analysis can only be carried out if the band bending can be determined. This fact has essentially eliminated the possibility of kinetic analysis for all systems where a change in the applied potential is partitioned between the two double layers and the band bending is unknown. In this section, we show how the partitioning of the applied potential influences current–potential curves at the semiconductor/solution interface.

From eq 10, it can be seen that as long as the current is a single-valued continuous function of the applied potential, the total differential of the current density,  $i$ , with respect to the applied potential,  $U$ , is given by

$$\frac{di}{dU} = \frac{\partial i}{\partial \Delta\phi_{\text{sc}}} \frac{\partial \Delta\phi_{\text{sc}}}{\partial U} + \frac{\partial i}{\partial \Delta\phi_{\text{H}}} \frac{\partial \Delta\phi_{\text{H}}}{\partial U} \quad (20)$$

For a semiconductor/solution interface, the overpotential (defined in the Butler–Volmer equation) is given by

$$\eta = \Delta\phi_{\text{H}} - \Delta\phi_{\text{H}}^{\text{eq}} \quad (21)$$

where  $\Delta\phi_{\text{H}}^{\text{eq}}$  is the electrostatic potential drop in the Helmholtz layer at the equilibrium potential. In addition, it can be seen that  $d(\Delta\phi_{\text{H}}) = d\eta$ .

From eq 20, it can be seen that there are two limiting cases for reactions at the semiconductor/solution interface: space charge layer control (first term on the right-hand side) and Helmholtz layer control (second term on the right-hand side). Below we only consider the situation for charge transfer from the conduction band to an electron acceptor in solution. A similar approach can be taken for the analysis of the current via the valence band for a p-type semiconductor.

The charge-transfer rate is determined by the overlap integral of the density of states of the electron acceptor in solution and the electron concentration at the surface of the semiconductor.<sup>4</sup> The reduction current due to majority carriers in the conduction band for an n-type semiconductor,  $i_{\text{cb}}$ , where the positions of the band edges are fixed is given by

$$i_{\text{cb}} = -ek_{\text{cb}}^- N_{\text{ox}} n_s \quad (22)$$

where  $k_{\text{cb}}^-$  is the potential-independent rate constant for reduction,  $N_{\text{ox}}$  is the density of electron acceptors in solution, and  $n_s$  is the electron concentration at the surface. The surface electron concentration is given by

$$n_s = N_D \exp\left(\frac{e\Delta\phi_{\text{sc}}}{kT}\right) \quad (23)$$

From eqs 22 and 23, it is seen that the rate constant can be obtained only if a plot of applied potential versus the logarithm of the current exhibits an inverse slope of 59 mV/decade at room temperature.

For the case where a change in the applied potential is dropped over the Helmholtz layer, the reaction rate can be described by the Butler–Volmer equation. At sufficiently large overpotentials where the oxidation reaction can be neglected, the current density is given by

$$i = -i_0 \exp\left(-\frac{\alpha_c e \eta}{kT}\right) \quad (24)$$

where  $\alpha_c$  is the cathodic transfer coefficient and  $i_0$  is the exchange current density.

Figure 9 shows the surface electron concentration,  $n_s$ , obtained from the band bending in Figure 3. From this figure, it is seen that  $n_s$  exhibits an inverse slope of 59 mV only at applied potentials positive to the flat band condition. As the potential is shifted negative of the flat band potential, the surface electron concentration increases more slowly and begins to saturate at an applied potential of about  $-0.2 \text{ V}$  (vs  $U_{\text{fb}}^0$ ). In this regime, the applied potential is partitioned between the space charge layer and the Helmholtz layer. At potentials negative to  $-0.4 \text{ V}$ , it can be seen from Figure 9 that  $n_s$  becomes almost independent of the applied potential as the band edges are almost completely unpinning. In this case, the reaction rate is expected to follow the Butler–Volmer model.

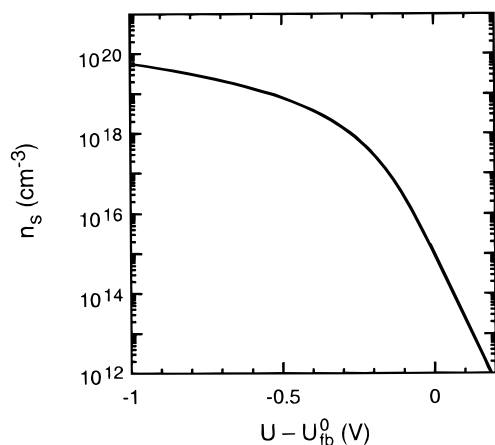


**Figure 9.** Surface electron concentration,  $n_s$ , calculated for  $\epsilon = 12$ ,  $N_D = 1 \times 10^{15} \text{ cm}^{-3}$ , and  $C_H = 1 \mu\text{F cm}^{-2}$ .

For the case where the applied potential is partitioned between the space charge layer and the Helmholtz layer, it can be shown from eqs 20 and 22–24 that

$$\frac{dU}{d(\log(i))} = \frac{2.303kT}{e} \frac{1}{\gamma_{ac} + \alpha_c(1 - \gamma_{ac})} \quad (25)$$

In deep depletion,  $\gamma_{ac} = 1$  and the slope is 59 mV/decade, corresponding to the potential dependence of the density of electrons at the surface given by the Boltzmann equation (see eq 23). In the limiting case where  $\gamma_{ac} = 0$ , i.e.,  $C_H \ll C_{sc}$ , the slope of the  $\log(i)$  versus potential plot is equal to  $(2.303kT/e\alpha_c)$  as defined in the Butler–Volmer equation (see eq 24). For intermediate cases, the slope increases from 59 ( $\gamma_{ac} = 1$ ) to 118 mV/decade (for  $\alpha_c = 0.5$ ). For example, in a situation where one-half of the applied potential is dropped over the Helmholtz layer ( $\gamma_{ac} = 0.5$ ) and  $\alpha_c = 0.5$ , the slope is equal to 80 mV/decade.

In the literature there have been relatively few studies of the kinetics of charge transfer at semiconductor surfaces in the dark. Morrison<sup>78</sup> and Gomes and co-workers<sup>79</sup> have reported on the reduction of  $\text{Fe}(\text{CN})_6^{3-}$  at n-type ZnO single crystals in aqueous solutions, and Fajardo and Lewis<sup>56</sup> have reported on the rate constants for the reduction of a range of viologen-based redox couples at n-type Si electrodes in methanol. In these cases, the current–potential curves were analyzed under depletion conditions with 0.2–0.6 V band bending. These groups all reported that the slopes of the current–potential curves were 65–66 mV, slightly larger than the theoretical value of 59 mV, suggesting that even under these nearly ideal conditions there is a small but measurable shift in the position of the band edges. From eq 25, it can be seen that for  $\alpha_c = 0.5$  and  $dU/d(\log(i)) = 65 \text{ mV/decade}$ , we obtain  $\gamma_{ac} = 0.85$ , consistent with Figure 2.

**Acknowledgment.** This work was supported by the U.S. Army Advanced Materials Research Collaboration Program (DAAL019620047). A.N. acknowledges helpful discussions with Dr. A. Worlikar.

## References and Notes

- (1) Myamlin, V. A.; Pleskov, Yu. V. *Electrochemistry of Semiconductors*; Plenum: New York, 1967.
- (2) Morrison, S. R. *Electrochemistry at Semiconductor and Oxidized Metal Electrodes*; Plenum: New York, 1980.
- (3) Pleskov, Yu. V.; Gurevich, Yu. Ya. *Semiconductor Photoelectrochemistry*; Consultants Bureau: New York, 1986.
- (4) Gerischer, H. *Electrochim. Acta* **1990**, *35*, 1677.

- (5) Mott, N. F. *Proc. R. Soc. (London) A* **1939**, *171*, 27.
- (6) Schottky, W. Z. *Phys.* **1939**, *113*, 367.
- (7) Many, A.; Goldstein, Y.; Grover, N. B. *Semiconductor Surfaces*; North-Holland Publishing Company: Amsterdam, 1965.
- (8) De Gryse, R.; Gomes, W. P.; Cardon, F.; Vennik, J. J. *Electrochem. Soc.* **1975**, *122*, 711.
- (9) Garrett, C. G. B.; Brattain, W. H. *Phys. Rev.* **1955**, *99*, 376.
- (10) Freund, T.; Morrison, S. R. *Surf. Sci.* **1968**, *9*, 119.
- (11) Dewald, J. F. *Bell Syst. Technol. J.* **1960**, *39*, 615.
- (12) Dewald, J. F. *J. Phys. Chem. Solids* **1960**, *14*, 155.
- (13) For solid-state junctions, the applied potential is usually referenced to the built-in potential. In semiconductor electrochemistry, the analogous situation would be the open-circuit potential for a semiconductor in equilibrium with an outer-sphere redox couple in solution. However, in many cases, these conditions are not achieved and the band bending under open-circuit conditions is not well-defined.
- (14) Note that if  $\Delta\phi_H = 0$  at  $U = U_{fb}^0$ , then  $\Sigma d\Delta(\phi_H(U)) = \Delta(\phi_H(U))$ . Physically, this describes the situation where the bands are flat ( $\Delta\phi_{sc} = 0$ ) and there is no charge on the surface. In the presence of surface states, adsorbates, or an interfacial layer, however,  $\Delta\phi_H \neq 0$  at  $U = U_{fb}^0$ . In this case, even though  $\Delta\phi_{sc} = 0$ , charge on the semiconductor surface induces a charge in the solution and a potential drop in the Helmholtz layer. If the additional charge on the surface (e.g., due to adsorbates) is independent of potential, a constant is added to the equations ( $\Delta\phi_H = \Delta\phi_H(U) + A$ ). However, if the magnitude of the additional charge is potential dependent (e.g., due to filling of surface states), then a potential-dependent term must be added ( $\Delta\phi_H = \Delta\phi_H(U) + A(U)$ ).
- (15) Gerischer, H.; Mauerer, A.; Mindt, W. *Surf. Sci.* **1966**, *4*, 431.
- (16) Memming, R.; Neumann, G. *J. Electroanal. Chem.* **1969**, *21*, 295.
- (17) Schröder, K.; Memming, R. *Ber. Bunsen-Ges. Phys. Chem.* **1985**, *89*, 385.
- (18) Vanmaekelbergh, D. *Electrochim. Acta* **1997**, *42*, 1121.
- (19) Vanmaekelbergh, D. *Electrochim. Acta* **1997**, *42*, 1135.
- (20) Kelly, J. J.; Memming, R. *J. Electrochem. Soc.* **1982**, *129*, 730.
- (21) Memming, R.; Schwandt, G. *Surf. Sci.* **1966**, *5*, 97.
- (22) Oskam, G.; Hoffmann, P. M.; Searson, P. C. *Phys. Rev. Lett.* **1996**, *76*, 1521.
- (23) Oskam, G.; Hoffmann, P. M.; Schmidt, J. C.; Searson, P. C. *J. Phys. Chem.* **1996**, *100*, 1806.
- (24) Bard, A. J.; Bocarsly, A. B.; Fan, F.-R. F.; Walton, A. G.; Wrighton, M. S. *J. Am. Chem. Soc.* **1980**, *102*, 3671.
- (25) Dittrich, Th.; Rauscher, S.; Bitzer, Th.; Aggour, M.; Flietner, H.; Lewerenz, H. *J. Electrochem. Soc.* **1995**, *142*, 2411.
- (26) Fantini, M. C. A.; Shen, W.-M.; Tomkiewicz, M. *J. Appl. Phys.* **1989**, *65*, 4884.
- (27) Nagasubramanian, G.; Wheeler, B. L.; Bard, A. J. *J. Electrochem. Soc.* **1983**, *130*, 1680.
- (28) Nicollean, E. H.; Goetzberger, A. *Bell Syst. Technol. J.* **1967**, *46*, 1055.
- (29) Goetzberger, A.; Klausmann, E.; Schulz, M. J. *CRC Critical Reviews in Solid State Sciences*; CRC Press: Boca Raton, FL, 1976; p 1.
- (30) Oskam, G.; Schmidt, J. C.; Hoffmann, P. M.; Searson, P. C. *J. Electrochem. Soc.* **1996**, *143*, 2531.
- (31) Matsumura, M.; Morrison, S. R. *J. Electroanal. Chem.* **1983**, *147*, 157.
- (32) Madou, M. J.; Frese, K. W.; Morrison, S. R. *J. Phys. Chem.* **1980**, *84*, 3423.
- (33) Madou, M. J.; Loo, B. H.; Frese, K. W.; Morrison, S. R. *Surf. Sci.* **1981**, *108*, 135.
- (34) Alberly, W. J.; O'Shea, G. J.; Smith, A. L. *J. Chem. Soc., Faraday Trans.* **1996**, *92*, 4083.
- (35) Bockris, J. O'M.; Reddy, A. K. N. *Modern Electrochemistry*; Plenum Press: New York, 1970; Vol. 2, p 753.
- (36) Gerischer, H.; Rosler, H. *Chem. Eng. Technol.* **1970**, *42*, 176.
- (37) Vanden Berghe, R. A. L.; Gomes, W. P. *Ber. Bunsen-Ges. Phys. Chem.* **1972**, *76*, 481.
- (38) Oskam, G.; Schmidt, J. C.; Searson, P. C. *J. Electrochem. Soc.* **1996**, *143*, 2538.
- (39) Schefold, J. J. *Electroanal. Chem.* **1992**, *341*, 111.
- (40) De Wit, A. R.; Vanmaekelbergh, D.; Kelly, J. J. *J. Electrochem. Soc.* **1992**, *139*, 2508.
- (41) Gomes, W. P.; Vanmaekelbergh, D. *Electrochim. Acta* **1996**, *41*, 967.
- (42) Dutoit, E. C.; Van Meirhaeghe, R. L.; Cardon, F.; Gomes, W. P. *Ber. Bunsen-Ges. Phys. Chem.* **1975**, *79*, 1206.
- (43) Gerischer, H.; McIntyre, R. J. *Chem. Phys.* **1985**, *83*, 1363.
- (44) Laflère, W. H.; Van Meirhaeghe, R. L.; Cardon, F.; Gomes, W. P. *Surf. Sci.* **1976**, *59*, 401.
- (45) Oskam, G.; Vanmaekelbergh, D.; Kelly, J. J. *J. Electroanal. Chem.* **1991**, *315*, 65 (and *J. Electroanal. Chem.* **1992**, *328*, 371).
- (46) Natarajan, A.; Oskam, G.; Searson, P. C. *J. Appl. Phys.* **1998**, *83*, 2112.
- (47) Koval, C. A.; Howard, J. N. *Chem. Rev.* **1992**, *92*, 411.

- (48) Smith, B. B.; Nozik, A. J. *J. Chem. Phys.* **1996**, 205, 47.
- (49) Miller, R. J. D.; McLendon, G. L.; Nozik, A. J.; Schmickler, W.; Willig, F. *Surface Electron-Transfer Processes*; VCH: New York, 1995.
- (50) Uhlendorf, I.; Reineke-Koch, R.; Memming, R. *J. Phys. Chem.* **1996**, 100, 4930.
- (51) Lewis, N. S. *Annu. Rev. Phys. Chem.* **1991**, 42, 543.
- (52) Tan, M. X.; Laibinis, P. E.; Nguyen, S. T.; Kesselman, J. M.; Stanton, C. E.; Lewis, N. S. In *Progress in Inorganic Chemistry*; Karlin, K. D., Ed.; Wiley: New York, 1994; Vol. 41, p 21.
- (53) Meissner, D.; Memming, R. *Electrochim. Acta* **1992**, 37, 799.
- (54) Memming, R. *Solid State Ionics* **1997**, 94, 131.
- (55) Nozik, A. J.; Memming, R. *J. Phys. Chem.* **1996**, 100, 13061.
- (56) Fajardo, A. M.; Lewis, N. S. *Science* **1996**, 274, 969.
- (57) Rosenbluth, M. L.; Lewis, N. S. *J. Am. Chem. Soc.* **1986**, 108, 4689.
- (58) Fan, F.-R. F.; Keil, R. G.; Bard, A. J. *J. Am. Chem. Soc.* **1983**, 105, 220.
- (59) Malpas, R. E.; Itaya, K.; Bard, A. J. *J. Am. Chem. Soc.* **1981**, 103, 1622.
- (60) Bard, A. J.; Bocarsly, A. B.; Fan, F.-R. F.; Walton, E. G.; Wrighton, M. S. *J. Am. Chem. Soc.* **1980**, 102, 3671.
- (61) Marcus, R. A. *Angew. Chem., Int. Ed. Engl.* **1993**, 32, 1111.
- (62) Marcus, R. A. *J. Chem. Phys.* **1956**, 24, 966.
- (63) Marcus, R. A. *Can. J. Chem.* **1959**, 37, 155.
- (64) Marcus, R. A. *J. Phys. Chem.* **1963**, 67, 853.
- (65) Marcus, R. A. *J. Chem. Phys.* **1965**, 43, 679.
- (66) Gerischer, H. Z. *Phys. Chem.* **1960**, 26, 223.
- (67) Gerischer, H. Z. *Phys. Chem.* **1960**, 26, 325.
- (68) Gerischer, H. Z. *Phys. Chem.* **1961**, 27, 48.
- (69) Gerischer, H. J. *Phys. Chem.* **1991**, 95, 1356.
- (70) Mollers, F.; Memming, R. *Ber. Bunsen-Ges. Phys. Chem.* **1972**, 76, 469.
- (71) Memming, R.; Mollers, F. *Ber. Bunsen-Ges. Phys. Chem.* **1972**, 76, 475.
- (72) Memming, R. *J. Electrochem. Soc.* **1978**, 125, 117.
- (73) Memming, R. *Ber. Bunsen-Ges. Phys. Chem.* **1987**, 91, 353.
- (74) Schmickler, W. *Ber. Bunsen-Ges. Phys. Chem.* **1978**, 76, 477.
- (75) Gomes, W. P.; Cardon, F. *Ber. Bunsen-Ges. Phys. Chem.* **1970**, 74, 431.
- (76) Tyagai, V. A.; Kolbasov, G. Ya. *Surf. Sci.* **1971**, 28, 423.
- (77) Lorenz, W.; Handshuh, M.; Bergmann, F. *Chem. Phys.* **1997**, 215, 139.
- (78) Morrison, S. R. *Surf. Sci.* **1969**, 15, 363.
- (79) Vanden Berghe, R. A. L.; Cardon, F.; Gomes, W. P. *Surf. Sci.* **1973**, 39, 368.